Acta Technica 62 (2017), No. 6B, 291–300

Classification and identification of pore structure and adsorption characteristics of liquid nitrogen in coal reservoir

Chuantao Wang[1], Yucheng Xia[1], Dongmin, Ma[2]

Abstract. This paper analyzes the law of different layers of coal layer pore characteristics of different regions, the specific surface area, adsorption curve and phase distribution of the pore configuration, specific surface area with FHH fractal features several aspects characterize the micropore characteristics of coal reserves. At the same time, the coal pore of low temperature nitrogen adsorption experiments were conducted respectively by liquid nitrogen surface data analysis of BET nano pore fractal characteristics of coal, the coal pore of low temperature nitrogen adsorption curve with the change of the coal rank, coal and mineral composition, microstructure of coal adsorption curve (Kong Jing structure) and FHH fractal features. Also known as the "relationship between the specific surface area pore structure of coal composition and chemical structure, and to classify and identify the adsorption curve. The fractal characteristics of the micro pore structure of the coal reservoir can comprehensively reflect the structural characteristics of the evolution of the micro porosity system of the coal reservoir with various factors, which may be the characteristic parameters of characterizing the micro pore system of the coal reservoir.

Key words. Classification and identification Pore structure Adsorption characteristics Coal reservoir FHH.

1. Introduction

In recent years, the in-depth study of coal reservoir exploration under the unconventional condition has been carried out step by step, and because of a large amount of coal resources stored in stratum of coal shale, more and more attention has been paid to it, and traditional understanding has been broken through. Many literatures

[1]School of geology and environment, Xi'An University of science and technology, Xi'An Shaanxi, 710054, China

are devoted to the study and analysis [1~2] of the pore characteristics of coal shale stratum in order to achieve the study for coal storage mechanism of coal shale stratum. The super compactness is the typical characteristic for coal reservoir of coal shale, the pore of coal shale has smaller pore structure comparing with carbonate rock and sandstone reservoir, of which the diameter can be up to Nanoscale. For instance, according to relevant study, it is reported that the pore diameter distribution scope of coal shale in coal stratum at Mississippian basin is 5~750nm, of which the mean value of pore diameter is 100nm, the pore diameter distribution scope of coal shale in coal stratum at Beaufort Mackenzie basin is 25~1000nm, the pore diameter of shallow coal shale in coal stratum at Haynesville basin is 20nm, however, the pore diameter of deep coal shale is 2.5~5nm. The pore diameter of coal shale with high maturity at coal exploration area of our country is about 15~100nm. The absorbability and reservoir properties of stratum to coal will be directly influenced by pore structure characteristics of coal shale, and at the same time the movement of coal will also be influenced [4].

In this paper, after disposing the surface of shale sample by liquid nitrogen adsorption and testing coal pore by low temperature nitrogen adsorption, mutual relation between "pore specific surface area—pore structure—coal material composition and chemical structure" is achieved, so as to obtain the structural features which can reflect the evolution of the micro pore system of coal reservoir with various factors, which may become characteristic parameters which characterize the micropore system in coal reservoir.

2. Experimental test

2.1. Testing materials

The test samples are collected from sample product of coal shale core of domestic coal mine. This sample is located in the Jurassic shale stratum, at the depth of 1800 meters underground, lift to surface through the crustal movement. The depth of shale core with 41~51m shall be searched, which is located in carbonate stratum, and it is the mature coal shale with vitrinite reflectance Ro of 0.88 %. The porosity is measured about 1%. The excellent bedding is shown in samples of dark gray to black, and the gray belt with the maximum thickness of 1mm is the embedded parallel melnikovite-pyrite.

The compressive strength (UCS) parallel to bedding is about 35%, less than that of vertical bedding (axis-Z direction) or obviously below that of oblique bedding (45° direction) which is about 48%. In the meantime, there is anisotropy on Young modulus, $E_{xy}/E_z = n \approx 1.7$. The Poisson's ratio is $v_{zy} = n \cdot v_{yz}$, of which v_{yz} is Poisson's ratio in the opposite direction of load and is a prerequisite condition for transversely isotropic elasticity. The shear modulus of normal coal shale bedding can be estimated to be $G_z = E_{xy}/(1 + n + 2nv_{zy})$.. Bedding shear modulus that is symmetry plane can be estimated to be $G_{xy} = E_{xy}/(2 + 2v_{xy})$.. The measured physical and mechanical parameters are respectively shown in Table 1 and Table 2.

Table 1. Test for physical parameters of coal shale reservoir

Maturity	0.88
Porosity (%)	1.1 ± 0.3
Average pore radius (nm)	< 4.1
Calcite content (wt %)	47.3 ± 0.5
Clay content (wt %)	27.8 ± 1.6
Quartz content (wt %)	17.2 ± 0.4
Pyrite (wt %)	5.3 ± 0.2
(wt%) Total organic carbon TOC (wt %)	5.8 ± 0.3
Water content (wt %)	~ 1

Table 2. Uniaxial compressive strength (UCS) and elastic property

E^a_{xy}	17.3 GPa	E^a_z	10.4 GPa
v_{xy}	0.18	v_{zy}	0.30
G_{xy}	8.9 GPa	G_z	5.5 GPa
UCS_{xy}	75 ± 7 MPa	UCS_z	115 ± 7 MPa
UCS_{45}	60 ± 10 MPa	v_{yz}	0.17
n	1.66		

2.2. Sample preparation

Under the drying condition, the cylindrical sample shall be drilled along bedding plane ($\alpha = 90^\circ - \beta$) of core materials with$\alpha \in [30^\circ, 86^\circ]$. The diameter of sample is 40mm, the length is 80mm and the precision is $< 20\mu m$ parallel to end face. Finally, the sample shall be drilled with drilling diameter of 8mm by solid carbon bit. The specific size of sample is shown in Table 3. The sample picture of coal shale collected from above four different areas is shown in Fig. 1, which shows the black coal shale at sampling point ① , with high carbon feature and containing Ostracoda, Thilobita and other biological fossil and the obvious sage green feature is shown in weathering part due to obvious trace of weathering. The sample is rich in organic matter, organic carbon content of more than 5%, but with low organic maturity. The sampling point ② also shows black coal shale sample, and content of trilobites as well as brachiopods fossils is abundant with small clumps and small spots locally, with fine bedding features and calcite veinlets filling, and weathering characteristics of coal shale is not obvious, and its maturity is between 2.5%∼2.7%, reaching a higher maturity. There is an obvious black compactness for coal shale of sampling point ③ , which contains higher siliceous, with more fractures developed and cemented by calcite, there is apparent bituminous material on the shale surface, the weathering of sample is not obvious and the sample has a higher maturity. The shale coal sample shown in sampling point ④ is brown, produced from stability sedimentary area under warm humid environment area of lacustrine facies and lacustrine, which is mainly coal shale of mud component. This peat shale is rich in organic matter content, between 0.76%~0.98%, with moderate degree of thermal evolution, and organic maturity is distributed between 2.2%~2.7%.

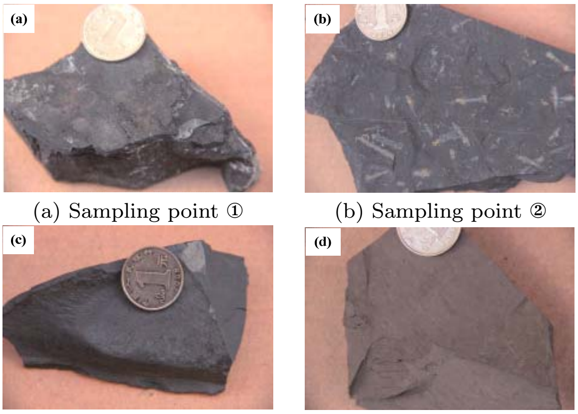

(a) Sampling point ① (b) Sampling point ②

(c) Sampling point ③ (d) Sampling point ④

Fig. 1. Sample picture of coal shale

3. Experimental analysis

3.1. Experiment for influencing factor of specific surface area and pore

There are a large number of nanopores developed in collected coal shale and Kerogen sample and the pore diameter distribution range from a few nanometers to hundreds of nanometers. Distribution curve for pore volume changing with pore diameter of different coal shale samples is shown in Fig.2a~Fig.2d. There is a certain similarity in coal shale of all sampling points with the distribution of pore diameter. It can be seen that the peak pore volume appears at the location with pore diameter around 6nm in the sampling point ① , which indicates that the number of micropores in the sampling point ① is dominant, similar to the results of above experiment. There are a number of "Peak" pore volume between the micropores and mesopores in the coal shale of sampling point ② , which indicates that the pore diameter of the coal shale in sampling point ② is mainly dominated by micropore and mesopore. Sampling point ③ is mainly dominated by the macropore coal shale, and the “Peak” pore volume appears in the 700nm, while in the micropores and mesopores, the change of pore volume is not obvious, and the number of nanopores in such section is limited. Feature of distribution curve of pore volume changing with pore diameter for coal shale in sampling point ④ is slightly different from sampling point ② , dominated by mesopores and supplemented by the number of micropores, which is related to developmental maturity of shale.

There is a certain difference in the specific surface area of Kerogen in different samples of coal shale mainly related to aperture size of Kerogen and influenced by type and maturity of organic matter. At the sampling point ① , the pore of kerogen is in immature development, and is in the original nonporous or micropore stage because it has not gone through expulsion and decomposition of hydrocarbon; the maturity of sampling point ② and sampling point ④ is relatively high, of which the kerogen after the expulsion and decomposition of hydrocarbon will enter into "gas window" of coal shale, to produce a large number of nanopores development, which can obviously improve porosity and specific surface area of coal shale. It is generally believed that a large number of nanopores can be produced only when the maturity reaches a certain value, which is related to the development and maturation of the nanopores inside the kerogen. For instance, in the literature [7], it is believed that a large number of nanoscale pores can be produced by secondary decomposition when the kerogen is in high maturity. In literature [8], based on the thermal simulation experiment of low-maturity coal shale samples, it is deduced that a large mount of development of manopores can be found inside the kerogen only when the temperature is heated to above 500°. There is a certain feature shown in the distribution of pore-pore volume when the kerogen is in the stage of over-maturity at sampling point ③ , but such feature is also related to the type of kerogen and other factors at the same time. The kerogen of sampling point ② and sampling point ④ is in the mature stage, however, the kerogen of sampling point ① is in immature stage, and the former kerogen has superior development of pore and specific surface area, and the experimental results show that the kerogen in this stage is prone to produce a large number of nanopores feature. In literature [9], the results show that the kerogen in mature stage has stronger coal adsorption properties than immature and overmature kerogen, which is in good agreement with the results presented in this study. In literature [10], the results show that the overmature kerogen has obvious aromatization characteristics and it is difficult to distinguish the type of kerogen due to more stable chemical structure. The pore volume and specific surface area of kerogen will not be affected by type, but related to component. Therefore, it is necessary to carry out in-depth experimental analysis and discuss when analyzing the pore structure of overmature kerogen.

3.2. Structural analysis of pore

According to the experimental data of liquid nitrogen adsorption, the calculation on the specific surface area of coal shale samples is shown in Table 3. The calculation range for specific surface area of above collected coal shale samples is 5.61∼10.20m2/g and the calculated mean value of the specific surface area is 8.38m2/g. The distribution range of the total pore volume of coal shale samples is 0.00675∼0.01297cm3/g and the calculated mean value is 0.00995cm3/g. The distribution range of the micropore volume of coal shale samples is 0.00052∼0.00122cm3/g and the calculated mean value is 0.00087cm3/g; the distribution range of the mesoporous volume of coal shale samples is 0.00463∼0.01029cm3/g and the calculated mean value is 0.00751cm3/g; the distribution range of the macropore volume of coal shale samples is 0.00116∼0.00202cm3/g and the calculated mean value is 0.00146cm3/g. The distribution range of pore diameter of coal shale samples is 2∼50nm mesopore,

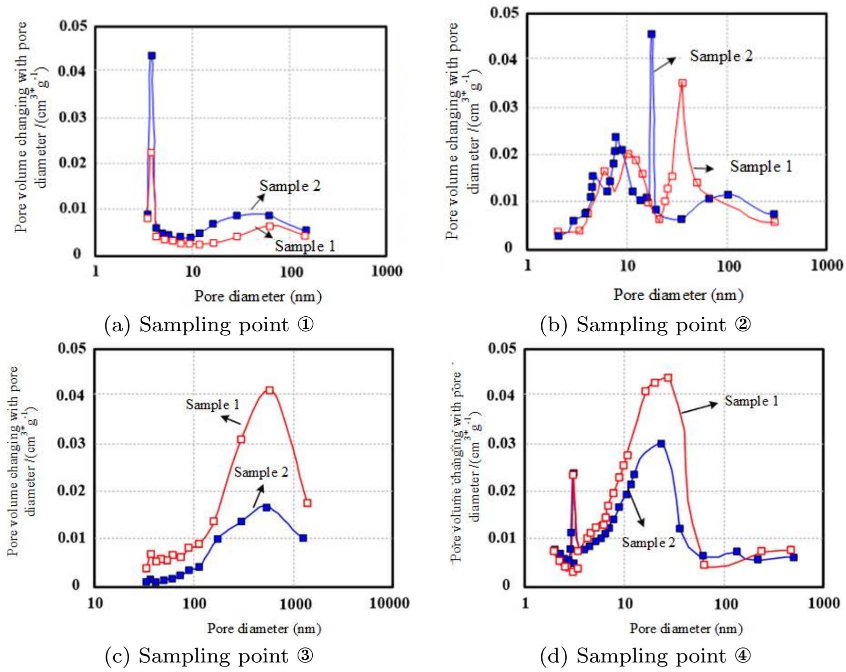

(a) Sampling point ①

(b) Sampling point ②

(c) Sampling point ③

(d) Sampling point ④

Fig. 2. Pore diameter distribution curve for different coal shale and kerogen

which is the main source of pore volume, to build main storage space of gas for coal shale.

Table 3. Calculation for pore diameter and specific surface area of coal shale

Sampling location	Sample	Specific surface area/(m2/g)	Average pore diameter/nm
Sampling point ①	Sample 1	7.30	19.68
	Sample 2	7.10	19.52
Sampling point ②	Sample 1	10.20	13.18
	Sample 2	9.42	13.24
Sampling point ③	Sample 1	5.61	25.14
	Sample 2	6.57	25.25
Sampling point ④	Sample 1	9.75	14.76
	Sample 2	9.26	14.62

3.3. Curve shapes for liquid nitrogen adsorption

The microcosmic size and connectivity of pore of coal shale samples can be greatly characterized by experimental curves of liquid nitrogen adsorption, and the experimental curve of liquid nitrogen adsorption for eight groups of above samples in total collected from sampling point ① ∼④ of domestic coal mine is shown in Fig.3.

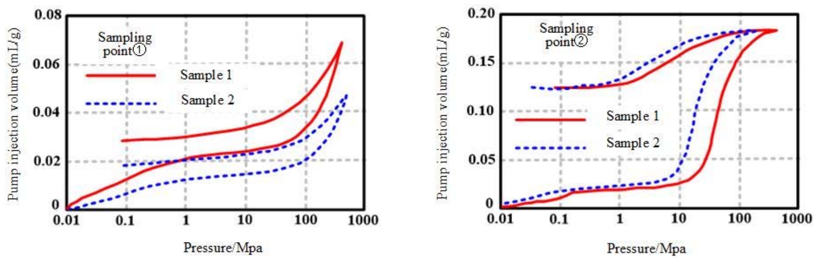

(a) Sampling point ① (b) Sampling point ②

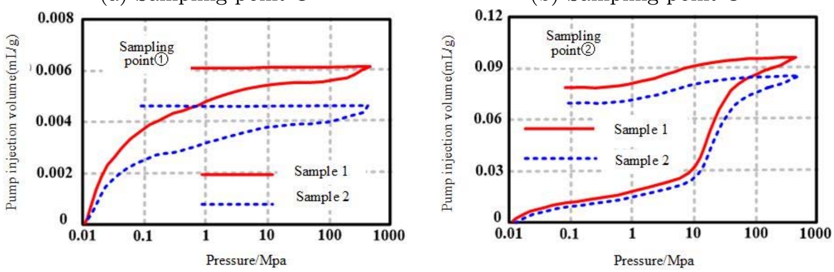

(c) Sampling point ③ (d) Sampling point ④

Fig. 3. Experimental curves for liquid nitrogen adsorption of coal shale

According to the experimental curves of liquid nitrogen adsorption of coal shale in Fig. 3, we can see that there are two types of liquid nitrogen adsorption modes in the experimental samples: (1) Immature mode (model I), (2) Mature mode (model II), (3) Overmature mode (model III). In model I, the volume change of liquid nitrogen adsorption is not obvious in the initial and medium stage of pressure increase, however that increases obviously in late stage of high pressure, mainly resulted from low sample maturity of sampling point ① , dominated by on micropores. In model II, with the increase of pressure, the volume change of liquid nitrogen adsorption in initial stage is not obvious, with very slow increase process, but with the increase of pressure, the volume change of liquid nitrogen adsorption increases rapidly in medium stage when pressure is higher than 10MPa, during which mercury injection volume can account for more than 50% of the total mercury volume and the mercury will exit quickly from pore of coal shale with the pressure reduction of mercury ejection. The differences between model I and model II are mainly reflected in that the pore at sampling point ① is mainly dominated by micropores, however, the pore of sampling point ② and sampling point ④ is mainly dominated by mesoporous and micropores with preferable connectivity. In model III, the volume of liquid nitrogen adsorption increases rapidly in initial stage of increasing initial pressure, but if increasing to l0MPa, the volume of liquid nitrogen adsorption changes vary slow, which shows that the shale sample is dominated by macropores. As shown in the experimental curves of liquid nitrogen adsorption in sampling point ③ , the differences of liquid nitrogen adsorption curves between model I, model II and model III are mainly related to the difference of pore feature in shale sample, mainly caused by the maturity of shale.

The result of above experiment shows that, the rapid change of liquid nitrogen adsorption volume and mercury ejection volume of model II after l0MPa indicates great pore structure development and connectivity of the shale sample in such model, and at the same time, for model I, the sample of coal shale has bad pore structure development and connectivity as well as poor coal storage property, however, for model III, the sample has oversize pore and poor absorbability for liquid nitrogen.

3.4. Fractal feature for FHH

The fractal model of coal shale pore is set up (see Fig.4). It can be seen from Fig.5, there is a significant fractal feature for pore of shale reservoir, and the correlation factors of sample are all above 0.96. The fractal dimension has a certain geological significance, and if fractal dimension is 3, corresponding to the volume filling, and is 2, corresponding to smooth surface without pore. If fractal dimension is between 2.760∼2.850, the sample has a minimum of pore space and has complex pore structure with powerful anisotropy.

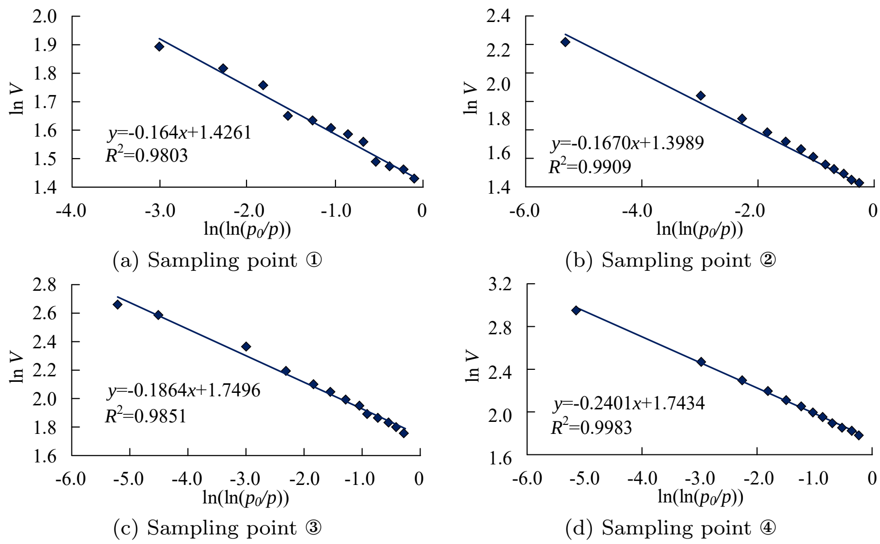

Fig. 4. Relation curve between different samples in experiment of low temperature nitrogen adsorption

The total pore volume, specific surface area of BET, average pore diameter and other pore structure parameter and the liner correlation between reservoir material component and fractal dimension are shown in Fig.5. It can be seen from Fig.5, there is a negative correlation between pore volume, average pore diameter and fractal dimension (see Fig. 5a∼ Fig. 5C), of which the negative correlation factor of pore volume and fractal dimension is 0.8669 and the negative correlation factor of average pore diameter and fractal dimension is 0.8982. There is a better positive correlation between the specific surface area of BET and fractal dimension, and the correlation factor is 0.935. The smaller the average pore size is, the smaller the pore

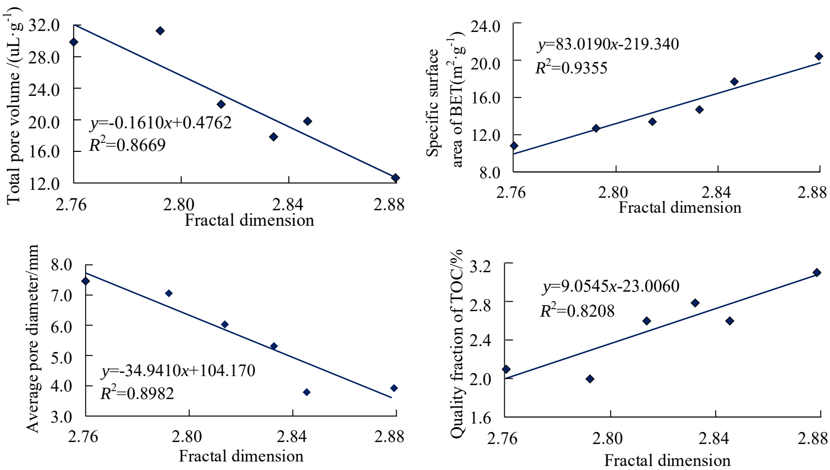

Fig. 5. Liner correlation between fractal dimension and pore structure parameter as well as reservoir material component

volume is and the larger the BET surface area is, the fractal dimension is closer to 3, which indicates that the pore volume, average pore diameter and specific surface area of BET in shale reservoir are important influencing factors for the fractal dimension of shale reservoir close to 3.

4. Conclusion

In this paper, based on the analysis of low temperature nitrogen adsorption experiment on the characteristics of coal reservoir, the experimental analysis from the index such as specific surface area, adsorption curve shapes, stage distribution of the pore structure, stage contribution of specific surface area of pore diameter and fractal feature of FHH is carried out to analyze BET fractal feature of coal nanopores, so as to get the change of low temperature nitrogen adsorption curve for coal pore with coal level, and the influence of coal micro composition and mineral composition on adsorption curve shapes (pore diameter structure) and FHH fractal feature, so that the structural features which can reflect the evolution of the micro pore system of coal reservoir with various factors are obtained, which may become characteristic parameters which characterize the micropore system in coal reservoir.

References

[1] Wang Y, Wang S, Wu G: (2014) *Pore characteristics of coal reservoir in Huhehu Depression and its effect on adsorption capacity*[J]. Fault-Block Oil & Gas Field, 585(3):331-336.

[2] Song X X, Tang Y G, Li W, et al.: (2013) *Fractal characteristics of adsorption*

pores of tectonic coal from Zhongliangshan southern coalmine[J]. Journal of China Coal Society, 38(1):134-139(6).

[3] Liu S Q, Sang S X, Liu H H, et al.: (2015) *Growth characteristics and genetic types of pores and fractures in a high-rank coal reservoir of the southern Qinshui basin*[J]. Ore Geology Reviews, 64(1):140-151.

[4] Bing L, Guocheng Z, Zhimin S, et al.: (2014) *Analysis on coupling relationship between pore structure of deformed coal and CH4 adsorption-desorption characteristics*[J]. International Journal of Earth Sciences & Engineering, 7(1):90-98.

[5] Zhang Z, Shi Y, Li H, et al.: (2016) *Experimental study on the pore structure characteristics of tight sandstone reservoirs in Upper Triassic Ordos Basin China*[J]. Energy Exploration & Exploitation, 34(3):418-439.

[6] Nie B, Liu X, Yang L, et al.: (2015) *Pore structure characterization of different rank coals using gas adsorption and scanning electron microscopy*[J]. Fuel, 158:908-917.

[7] Liu S Q, Sang S X, Liu H H, et al.: (2015) *Growth characteristics and genetic types of pores and fractures in a high-rank coal reservoir of the southern Qinshui basin*[J]. Ore Geology Reviews, 64(1):140-151.

[8] Bing L, Guocheng Z, Zhimin S, et al.: (2014) *Analysis on coupling relationship between pore structure of deformed coal and CH4 adsorption-desorption characteristics*[J]. International Journal of Earth Sciences & Engineering, 7(1):90-98.

[9] Zhang Z, Shi Y, Li H, et al.: (2016) *Experimental study on the pore structure characteristics of tight sandstone reservoirs in Upper Triassic Ordos Basin China*[J]. Energy Exploration & Exploitation, 34(3):418-439.

[10] Yang W, Zhu Y, Chen S, et al.: (2014) *Characteristics of the Nanoscale Pore Structure in Northwestern Hunan Shale Gas Reservoirs Using Field Emission Scanning Electron Microscopy, High-Pressure Mercury Intrusion, and Gas Adsorption*[J]. Energy Fuels, 28(2):945-955.

[11] Tang S H, Zhang J P, Min-Jie W U: (2013) *The Pore Structure Characteristic about the Sapropelic Coal*[J]. Natural Gas Geoscience, 24(2):247-251.

Received May 7, 2017